Journal of Physics and Its Applications

Journal homepage : https://ejournal2.undip.ac.id/index.php/jpa/index

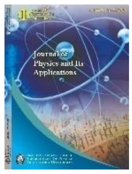

Design of Radiation Shielding in X-Ray Rooms: A Study on Radiological Protection

Aditya S. Hartanti[1,3], Chomsin S. Widodo[1], Zaenal Arifin[2], Johan Andoyo E. Noor[3*]

[1]Department of Physics, Brawijaya University, Malang, Jawa Timur, Indonesia
[2]Department of Physics, Diponegoro University, Semarang, Jawa Tengah, Indonesia
[3]Department of Radiology, Karsa Husada Regional Public Hospital, Batu, Jawa Timur, Indonesia

**Corresponding author : jnoor@ub.ac.id*

ARTICLE INFO

Article history:
Received: 28 May 2025
Accepted: 21 November 2025
Available online: 27 February 2026

Keywords:
Radiation shielding
X-ray room design
Radiation Safety Standard
Radiation absorbing materials

ABSTRACT

Radiation exposure protection is a critical aspect in the utilization of X-ray technology in the medical field. An effective radiation shielding design in X-ray rooms is not only important to protect patients, but also to ensure the safety of medical personnel who are routinely exposed to radiation. Alongside advancements in medical imaging technology, the design of X-ray rooms and shielding system continue to evolve to meet increasingly stringent safety standards. This article aims to review recent approaches in radiation shielding design for X-ray rooms, with a focus on improving radiological protection. The study covers various materials used for shielding, such as lead, concrete, and alternative environmentally friendly materials, as well as new technologies in radiation protection systems. Additionally, it highlights optimal X-ray room design techniques, such as the placement of X-ray equipment, distance management, and room configuration, to minimize radiation exposure to unintended areas. Challenges in implementing shielding designs, including cost, space limitations, and compliance with safety regulations, are also thoroughly discussed. Furthermore, this article identifies the need for further research in this field, particularly regarding the development of more efficient and affordable shielding materials, as well as more innovative design approaches. The findings of this study are expected to provide new insights and practical recommendations that can be used by medical professionals, medical facility designers, and policymakers to enhance radiation safety standards in healthcare facilities.

1. Introduction

Exposure to ionizing radiation in medical imaging facilities remains a critical concern due to its potential long-term biological effects. Continuous low-dose radiation exposure may increase cancer risk, particularly among medical personnel who are frequently exposed in clinical settings [1]. Although mitigation efforts have been implemented, such as the use of artificial intelligence (AI)-based dosimeters for real-time monitoring [2] and educational programs aimed at reinforcing the As Low As Reasonably Achievable (ALARA) principle among healthcare workers [3], uncontrolled exposure still poses a challenge in high-workload environments [4]. Therefore, an effective and well-designed shielding system is essential to ensure the protection of patients, workers, and the public from radiation hazards [5].

Over time, various strategies have been developed to optimize shielding design in X-ray rooms [6]. The fundamental principles of radiation protection; time, distance, and shielding remain the primary guideline for reducing radiation exposure, in accordance with recommendations from the International Commission on Radiological Protection. Furthermore, the National Council on Radiation Protection and Measurements (NCRP) has issued detailed technical guidance through NCRP Report No. 49 and NCRP Report No. 147, which provide practical frameworks for the safe and efficient design of radiological facilities [7]. In Indonesia, radiation protection and facility design are regulated by the Nuclear Energy Regulatory Agency (BAPETEN) through Head of BAPETEN Regulation No. 8 of 2011 on Radiation Safety in Diagnostic and Interventional Radiology, as well as by the Ministry of Health through Regulation No. 1014/MENKES/PER/V/2011 [8]. These regulations reinforce the application of the ALARA principle, the implementation of shielding designs that meet safety standards, and the importance of continuous radiation monitoring in healthcare settings.

Despite the availability of regulatory frameworks and design methodologies, several scientific and technical issues remain insufficiently addressed. Differences between earlier shielding standards, such as NCRP 49 and more recent guidelines like NCRP 147, have resulted in inconsistent application, particularly regarding workload calculation, use factor, and source-to-wall distance [9]. Additionally, numerous studies have investigated innovative shielding materials such as barium-based concrete [10], environmentally friendly metal polymers [11], and tungsten-based elastomers [12], yet no comprehensive synthesis has evaluated their shielding effectiveness, optimal thickness, and practical feasibility in clinical environments. Simulation-based approaches such as Monte Carlo methods [13] and finite element analysis (FEA) [14] have also been used to model radiation distribution and determine barrier thickness; however, practical guidance on how to translate these simulation results into real-world shielding design remains limited [15]. Moreover, recent developments in modular and lightweight shielding technologies, such as graphene-based panels [16] and lead–polymer composites [17], present new opportunities, but their integration within existing standards and clinical workflows requires further investigation from the perspectives of performance, sustainability, and adaptability.

International guidelines from the British Institute of Radiology (BIR) 14 and the International Atomic Energy Agency (IAEA) offer additional perspectives on material selection, design efficiency, aesthetic considerations, and staff training. Nevertheless, no existing review has systematically compared and integrated these guidelines with national regulations, technological advancements, and evolving clinical demands [18]. This reveals a knowledge gap in how fundamental radiation protection principles, material innovations, simulation-based design techniques, and regulatory frameworks can be synthesized into a comprehensive and practical shielding design approach. To address this gap, this study explores the latest trends in X-ray shielding design, evaluates the effectiveness of traditional and novel shielding materials, examines the implementation of international and national standards in practical settings, and identifies how literature-based insights can be translated into practical guidance for facility design. The practical guidance proposed in this article includes criteria for selecting materials based on radiation energy and barrier location, design considerations incorporating workload, distance, and occupancy, integration of simulation tools such as Monte Carlo and FEA, recommendations for applying regulatory standards, and a step-by-step framework for designing shielding in various radiological procedures, including CT scan, mammography, panoramic imaging, and catheterization laboratories.

Therefore, this article aims to provide a comprehensive synthesis of recent developments in X-ray shielding design encompassing material innovations, design techniques, implementation of safety standards, and the development of practical guidance based on current literature in order to optimize safety, efficiency, and sustainability in modern radiology facilities.

2. Methods

Several methods for calculating shielding thickness in X-ray rooms have been developed and are widely applied in various international standards and guidelines. Some of the commonly used methods include:

2.1 Kerma and Effective Dose Method

The shielding thickness calculation method based on Kerma (Kinetic Energy Released per unit Mass) and effective dose is one of the most widely applied approaches in radiation protection because it integrates the physical energy transferred from photons to matter with the biological significance of radiation exposure in humans [19], enabling the conversion of source output and attenuation properties into predicted doses behind shielding barriers. Kerma, expressed in gray (Gy), quantifies the kinetic energy imparted per unit mass of material and is mathematically defined as

$$K = \frac{dE_{tr}}{d_m} \tag{1}$$

where dE_{tr} is the transferred energy and d_m is the mass of the absorbing material. In shielding design, air kerma is commonly used to characterize unshielded radiation at a reference point, which is then attenuated through shielding materials according to the exponential attenuation law

$$K(x) = K_0 e^{-\mu x} \tag{2}$$

where K_0 is the incident kerma, μ is the linear attenuation coefficient (cm^{-1}), and x is the shield thickness (cm). Alternatively, attenuation may be expressed using half-value layer (HVL = ln2/μ) or tenth-value layer (TVL = ln10/μ), allowing thickness to be determined using

$$x = TVL \cdot log_{10}(\frac{1}{B}) \tag{3}$$

where B is the required transmission factor.

To relate physical attenuation to biological safety, the method incorporates effective dose (E), which accounts for tissue radiosensitivity and reflects potential health risk. Effective dose is calculated from organ dose D_T and radiation weighting factor w_R, typically 1 for diagnostic X-rays, using

$$H_T = w_R D_T \text{ and } E = \textstyle\sum_T w_T H_T \tag{4}$$

where w_R is the tissue weighting factor. In practical shielding calculations, air kerma at a given point is converted to effective dose using tabulated or simulated conversion coefficients (μSv per μGy) that depend on photon energy and exposure geometry. Design goals set maximum permissible effective dose at the occupied area behind the barrier (e.g., 0.1 mSv/week for controlled or 0.02 mSv/week for uncontrolled areas), and barrier transmission is calculated using a standard relationship derived from NCRP-style formalism:

$$B = \frac{P \cdot d^2}{W \cdot U \cdot T} \tag{5}$$

where P is the permissible dose at the point of interest, d is the distance from source to that point, W is workload, U is the use factor (fraction of workload directed toward the barrier), and T is the occupancy factor. Once B is obtained, the shield thickness is calculated using either TVL, HVL, or attenuation coefficients. These equations provide a direct link between source output, geometry, operational parameters, biological dose limits, and required shielding thickness, forming the theoretical basis of the Kerma–effective dose method.

Several studies have demonstrated the practical application of the Kerma–effective dose method in determining optimal shielding thickness. Research findings indicate that lead provides the lowest kerma and transmission values up to 150 kVp, making it the most effective material at high energies [20]. Clinical investigations show that a thickness of 1.5–2 mm of lead can maintain effective doses below regulatory limits for both patients and staff, while simulation studies confirm that 2 mm of lead can reduce exposure by nearly 90% compared to no shielding [21, 22]. Other evaluations on repeated imaging procedures reveal that optimizing lead thickness can lower cumulative doses by about 75% without compromising image quality [23]. Validation using Monte Carlo analysis also shows a strong correlation between calculated and measured Kerma values, reinforcing the reliability of simulation-based shielding design [24, 25].

However, the required shielding thickness depends strongly on parameters such as X-ray energy range, source-to-barrier distance, and workload. Higher kVp values decrease attenuation coefficients and increase HVL or TVL, necessitating thicker barriers. Thus, the design energy should reflect the maximum operational voltage for safety, while the shortest practical source-to-wall distance should be applied to represent realistic exposure conditions. Workload, use, and occupancy factors need to be selected conservatively or based on clinical data [9]. Primary and secondary radiation must also be treated separately, as scattered beams have lower energy spectra and different HVL or TVL characteristics [19].

In summary, the Kerma–effective dose method provides a robust and validated framework for shielding design by integrating physical attenuation principles with biological safety criteria. Lead remains the preferred material because of its superior attenuation capability, while concrete and polymer composites are commonly used as structural or secondary barriers [26]. Supported by Monte Carlo verification and in line with WHO and national safety regulations, this method ensures accurate, efficient, and regulation-compliant radiation protection in diagnostic facilities [27].

2.2 Excel Spreadsheet or Online Calculator Models

Excel-based spreadsheets and online calculators have become practical tools for estimating shielding thickness when advanced simulation software is unavailable. These applications integrate key radiation protection parameters such as X-ray energy, source distance, workload, and exposure time, to calculate required shielding [28]. Most are based on the exponential attenuation equation,

$$I = I_0 e^{-\mu t} \tag{6}$$

where I is the transmitted intensity, I_0 is the incident intensity, μ is the linear attenuation coefficient of the material (which varies with energy), and t is the shielding thickness. Rearranging yields

$$t = \frac{-\ln\left(\frac{I}{I_0}\right)}{\mu} \tag{7}$$

allowing users to input transmission factors or permissible doses to obtain the necessary thickness. Excel templates and web-based versions have been developed to estimate lead or concrete thickness for simple geometries and to calculate Kerma and dose at various distances [29].

Several evaluations confirmed that such calculators provide results close to Monte Carlo simulations for X-ray energies below 100 kVp, with deviations under 10% [30]. However, accuracy decreases for complex geometries and non-uniform radiation fields due to simplifications in geometry and attenuation data [31]. Studies also highlight that integrating computational methods with empirical validation enhances design accuracy and efficiency [21].

To correctly apply this method, users should follow a structured procedure: (1) define the clinical workload and use factor, (2) determine energy range and select appropriate attenuation coefficients or tenth-value layers (TVL) from published databases, (3) calculate unshielded dose at the point of interest using inverse square law

$$D = D_0 \left(\frac{d_0}{d}\right)^2 \tag{8}$$

and (4) verify compliance with NCRP 147 and IAEA standards. Lead remains the preferred material up to 150 kVp due to its high density and low TVL, while concrete offers a cost-effective option for thicker structural barriers.

In summary, spreadsheets and online calculators provide quick, transparent, and accessible tools for preliminary shielding design. When validated with regulatory data and supported by appropriate safety margins, they can effectively complement advanced simulation approaches in ensuring radiation protection reliability.

2.3 International Standards: NCRP and ICRP

International standards from the NCRP, ICRP, BIR, and IAEA form the foundation for X-ray shielding design, each emphasizing radiation safety through different approaches and parameters. The NCRP model, particularly in Report No. 147, applies a workload-based framework that considers weekly radiation output, use and occupancy factors, and source-to-barrier distance. The permissible dose (P) determines the required transmission factor (B), which is converted into thickness using tenth-value layer (TVL) or attenuation data, providing conservative estimates suitable for high-dose settings such as interventional radiology [32]. Studies have confirmed that NCRP's workload model aligns well with the physical attenuation principles [5].

The ICRP framework, outlined in Publication 103, emphasizes biological protection by limiting effective dose to workers and the public through tissue weighting factors and dose conversion coefficients. Studies show that a 2 mm lead barrier maintains effective doses within limits at a 3 m distance from the X-ray source [33]. The BIR approach offers a simplified model using standardized attenuation data and typical workloads for 40–150 kVp, enabling manual or spreadsheet-based application [34], though it may be less accurate for non-standard geometries. Meanwhile, the IAEA Safety Reports Series combines NCRP's quantitative and ICRP's biological principles, showing results consistent with NCRP up to 120 kVp [35], while NCRP remains more conservative at energies above 150 kVp [36].

Key distinctions among these models involve treatment of energy, distance, and attenuation. NCRP and IAEA explicitly include source-to-barrier distance, whereas ICRP embeds it in dose conversion, and BIR assumes fixed layouts. NCRP uses energy-dependent TVL data, ICRP relies on dose coefficients, BIR employs standardized tables, and IAEA allows local attenuation data. To ensure consistency, users should (1) verify energy ranges match equipment specifications, (2) measure source-to-barrier distances accurately, (3) apply use and occupancy factors per barrier type, and (4) validate thickness with reliable attenuation or TVL data for materials like lead or concrete.

From a practical standpoint, the NCRP method offers the highest safety margin and is recommended for high-dose environments or when regulatory compliance requires conservative design. The ICRP method provides biologically relevant dose-based protection but may require more complex dose modeling. The BIR method is advantageous in resource-limited settings due to its simplicity, while the IAEA method provides international adaptability by integrating flexibility with technical rigor. Complementary national guidelines, such as Indonesia's Ministry of Health Regulation No. 1014/MENKES/PER/V/2011, further ensure compliance with patient safety standards [8]. Recent computational tools, including Excel-based shielding calculators [28], have facilitated the practical implementation of these standards, aligning well with WHO recommendations on safe radiology facility design [5]. In practice, NCRP offers the most conservative protection, ICRP emphasizes biological dose relevance, BIR supports rapid estimation, and IAEA provides international adaptability. When integrated appropriately, these frameworks enable accurate, safe, and efficient shielding design consistent with evolving clinical technologies.

2.4 Shielding Calculation Based on the Law of Attenuation

The Law of Attenuation is one of the most fundamental principles used to calculate the reduction of X-ray intensity as it passes through a shielding material. The relationship between the initial radiation intensity and the transmitted intensity after passing through a material of a given thickness is expressed mathematically by the exponential attenuation equation:

$$I = I_0 e^{-\mu x} \tag{9}$$

Equation [9] states that the transmitted intensity I is equal to the initial unshielded intensity I_0 multiplied by the exponential of the negative product of the linear attenuation coefficient μ and the material thickness x. In this context, I and I_0 are measured in watts per square meter ($W{\cdot}m^{-2}$), x represents the physical thickness of the shielding material in meters (m), and μ represents the attenuation coefficient of the material in inverse meters (m^{-1}), which quantifies how strongly the material absorbs or scatters the radiation. In other words, the greater the value of μ, the more quickly radiation intensity decreases as it travels through the material.

Compared with guideline-based methods such as NCRP 147 or IAEA models, which include workload, distance, and occupancy factors, the attenuation law focuses solely on exponential decay in a homogeneous medium. Thus, it provides a theoretical minimum thickness that may underestimate shielding needs if scatter and leakage are ignored. Nevertheless, it remains a practical foundation for simplified analytical models and educational applications [37]. However, the attenuation law offers a simple and transparent mathematical basis that is often used as the foundation upon which more complex standards are built.

To apply the attenuation law in practice, the user must first determine the initial intensity or dose rate at the barrier based on the X-ray tube output. Next, the acceptable transmitted intensity or design limit (e.g., permissible dose beyond the barrier) must be defined. The linear attenuation coefficient for the chosen material at the relevant X-ray energy must then be obtained from experimental data or published databases. By rearranging Equation (1), the required shielding thickness can be calculated using:

$$x = -\frac{1}{\mu} ln\left(\frac{I}{I_0}\right) \quad (10)$$

Equation [10] demonstrates that the thickness x is directly influenced by the ratio of allowable transmitted intensity to initial intensity and inversely proportional to the attenuation coefficient. Therefore, any variation in X-ray energy (which affects μ) or clinical workload (which affects I_0) will significantly influence the resulting shielding thickness.

To use this method effectively, readers should follow several practical steps. First, accurate input parameters such as X-ray energy spectrum, source to barrier distance, and exposure conditions must be defined to ensure realistic calculations. Second, attenuation coefficients should be selected from reliable sources and matched to the specific energy range of interest. Third, because the attenuation law does not inherently account for scattered or leakage radiation, additional correction factors may be necessary, or the results should be validated using more comprehensive models or simulation techniques such as Monte Carlo. Finally, the calculated thickness should be cross-checked against established international standards (e.g., NCRP 147 or ICRP recommendations) to ensure regulatory compliance and sufficient safety margins.

In summary, while the attenuation law offers a clear mathematical foundation for shielding calculation, it must be supplemented with clinical parameters and validated against regulatory standards (e.g., NCRP, WHO) to ensure adequate protection and compliance [37].

2.5 Monte Carlo Method

The Monte Carlo method is a probabilistic simulation technique that models photon–matter interactions by tracking millions of individual particle histories. Unlike analytical or empirical methods such as NCRP, ICRP, or BIR-based approaches that depend on predefined parameters (e.g., occupancy, workload, use factor) and tabulated transmission data, Monte Carlo simulations compute radiation transport statistically within complex geometries [6]. Analytical approaches like the exponential attenuation law assume narrow beams and homogeneous materials, whereas empirical or spreadsheet models simplify real conditions and may underestimate scatter and leakage effects [11].

Monte Carlo simulation explicitly reproduces primary, scattered, and leakage radiation in three dimensions, enabling accurate dose mapping for irregular barrier shapes, oblique angles, and secondary reflections. This allows for realistic shielding optimization, eliminating excessive conservatism while maintaining safety margins. However, this accuracy requires substantial computational power and specialized expertise, which makes the method more suitable for advanced design verification rather than routine layout calculations [38].

Reliable implementation depends on several critical factors, including accurate source modeling (X-ray energy spectrum, filtration, workload), precise room geometry, correct material composition and density, and appropriate physics transport settings. The number of simulated particle histories determines statistical convergence, while variance reduction techniques (e.g., splitting or importance sampling) improve computational efficiency. Validation against benchmark experiments or standard reference data remains essential to ensure accuracy and regulatory compliance [39].

In summary, the Monte Carlo method provides superior precision and flexibility compared with analytical or empirical models. When properly configured and validated, it serves as an indispensable tool for optimizing radiation shielding in medical imaging facilities, supporting safe and efficient room design in accordance with modern safety standards.

3. Result and Discussion

3.1 Factors Affecting Shielding Calculations

The factors mentioned are essential elements in shielding thickness calculations for radiation protection. Each plays a critical role in determining the required level of shielding to ensure safety for patients, medical staff, and the surrounding environment.

3.1.1 Type and Energy of Radiation

This study focuses on diagnostic X-ray applications commonly used in clinical practice, including radiography (40–120 kVp), fluoroscopy (70–110 kVp), computed tomography (80–140 kVp), and interventional radiology (up to 150 kVp). Each modality requires specific shielding designs due to energy-dependent attenuation behavior. Prior research consistently shows that higher-energy X-rays penetrate materials more effectively, demanding thicker barriers to maintain the same dose reduction. Lead remains the most efficient attenuator, requiring 1.5–3 cm thickness depending on beam energy [40]. This illustrates a direct correlation between tube potential (kVp) and shielding needs. Studies also indicate that higher-energy procedures such as interventional radiology and CT require thicker protection than conventional radiography [41], recommending the use of dense materials such as lead or heavy concrete adjusted for energy, distance, and room occupancy to comply with dose limits. The study in [42] further confirmed lead's superior attenuation compared to concrete or other low-density materials, supporting its continued use for high-energy shielding.

International standards, including NCRP Report No. 147 and the IAEA Safety Series, define two key parameters: the half-value layer (HVL) and tenth-value layer (TVL). HVL represents the material thickness reducing beam intensity by 50%, while TVL reduces it by 90%. As X-ray energy increases, both values rise, reflecting reduced attenuation efficiency at higher photon energies. Representative TVL values for lead and standard concrete used in diagnostic shielding are shown below at table 1.

Table 1: TVL values for lead and standard concrete at diagnostic X-ray energies

X-ray Tube Potential (kVp)	TVL for Lead (mm)	TVL for Concrete (cm)
80 kVp	~0.5–0.7 mm	~3–4 cm
100 kVp	~0.8–1.0 mm	~5–6 cm
120 kVp	~1.2–1.5 mm	~6–8 cm
150 kVp	~1.5–2.0 mm	~8–10 cm

These values show that required thickness increases proportionally with beam energy. In practical design, the number of TVLs needed to reach acceptable dose levels is determined by workload, use factor, occupancy, and distance, following NCRP 147 and IAEA methods. For instance, achieving a 0.1% transmission level requires approximately three TVLs of shielding [43]. The choice between lead and concrete depends on structure, cost, and desired attenuation.

In application, designers must identify the X-ray type and tube potential, reference HVL or TVL data, and calculate the total shielding thickness to meet dose limits. Distance from source and scattered radiation paths must also be evaluated since greater distance reduces barrier exposure. A safety margin should be added to account for construction and beam variability. Integrating TVL data with workload and room geometry yields accurate, standardized, and regulation-compliant shielding thicknesses, ensuring optimal radiation protection across diagnostic X-ray facilities.

3.1.2 Type of X-rays and Energy-Dependent Shielding Requirements

This study focuses on diagnostic X-rays generated by Multislice Computed Tomography (MSCT), specifically 128-slice CT scanners, which typically operate at 100–140 kVp. Compared to general radiography (70–100 kVp), CT scanners produce higher-energy photons, increased workloads, and 360° scatter radiation due to continuous gantry rotation. Consequently, shielding design in CT rooms primarily targets secondary radiation (scatter and leakage) rather than direct primary beams, most [44].

The energy of the X-ray beam strongly influences the half-value layer (HVL) and tenth-value layer (TVL) of shielding materials. Higher photon energies have greater penetration and require thicker shielding to achieve the same level of attenuation [45]. For example, lead thickness requirements have been reported to range from 1.5 to 3.0 cm as energy increases [46], while the use of heavy concrete or lead with thicknesses adapted to tube voltage and material attenuation properties has also been recommended [47]. Furthermore, gamma radiation has been shown to require even thicker shielding than X-rays of similar nominal energy, emphasizing the importance of differentiating radiation types in shielding design [48].

Table 2: Shielding Thickness Requirements as X-ray Energy Increases in Clinical Practice

Tube Voltage (kVp)	Typical Clinical Modality	Shielding Type	Approx. HVL (mm Pb)	Lead Thickness (mm)	Concrete Equivalent (cm)	References
70–80 kVp	Extremity/Pediatric Radiography	Secondary	0.25–0.30	1.0 – 1.5	6 – 8	(Bibbo, G., et al., 2017) [49]
90–100 kVp	General Radiography (abdomen/pelvis)	Primary+ Secondary	0.32–0.38	1.5 – 2.0	8 – 10	(Yusuf, S. D., et al.,2020) [50]
110–120 kVp	High-output Radiography/Low-Energy CT	Secondary	0.40–0.50	2.0 – 2.5	10 – 12	(Demirel, I., 2024) [16]
120–130 kVp	Standard MSCT (64–128 slice)	Secondary (dominant)	0.50–0.60	2.5 – 3.0	12 – 15	(Kim, S. C., et al., 2013) [34]
130–140 kVp	High-power MSCT (128–256 slice)	Secondary+ occasional primary	0.60–0.70	3.0 – 3.5	15 – 18	(Gupta, S., et al., 2022) [15]
>140 kVp	Interventional CT / Hybrid Angio-CT	Primary+ Secondary	>0.70	3.5 – 4.5+	18 – 22+	(Neeman, Z., et al., 2006) [45]

In clinical settings, shielding requirements are not determined by energy alone. They are also influenced by source-to-barrier distance, room geometry, workload (mA·min/week), occupancy factor (T), and barrier type (primary vs. secondary) [49, 50, 51]. For example, doubling the source-to-occupancy distance can reduce exposure by approximately 75%, thereby decreasing the required shielding thickness [55]. Consequently, computed tomography (CT) rooms with high workloads and full occupancy (T = 1.0) typically require thicker protective barriers than standard radiography rooms.

To provide a quantitative guideline, table 2 presents representative shielding thickness values for lead and concrete at different tube voltage ranges commonly used in diagnostic imaging. These data synthesize findings from previous studies and international guidelines to illustrate the general trend that as X-ray energy increases from 80 to 140 kVp, required shielding thickness increases from ∼1 mm to >3.5 mm of lead, or from ∼6 cm to >18 cm of concrete. This table serves as an initial reference before applying detailed calculations using NCRP 147, IAEA, or BIR methods, adjusted for specific clinical parameters such as geometry, occupancy, and workload.

3.1.3 Radiation Source Distance

Distance from the X-ray source to surrounding structural barriers is a critical parameter in shielding design, as radiation intensity decreases proportionally to the inverse square of the distance. Increasing the source-to-occupant distance significantly reduces the received dose, reinforcing the inverse square law as a fundamental principle of radiation protection [49]. Similarly, doubling the distance from the X-ray source can reduce the radiation dose by approximately 75% [51]. Thereby lowering the shielding thickness required to comply with dose limits. These findings highlight that strategic room layout and proper placement of the X-ray tube can minimize exposure to adjacent areas and reduce reliance on excessively thick shielding.

In clinical practice, ideal source-to-barrier distances vary depending on the modality and room design. For general diagnostic radiography rooms, the distance between the X-ray tube and the primary barrier (e.g., wall behind the bucky) typically ranges from 2.0 to 3.0 meters, allowing sufficient attenuation and compliance with NCRP 147 guidelines. In computed tomography (CT) rooms, the distance from the gantry to surrounding walls is commonly 1.5 to 2.5 meters, as CT systems emit a rotating fan beam with lower scatter intensity compared to fixed-beam radiography. For interventional suites, where operators remain inside the room during exposure, a greater separation is recommended; the distance between the isocenter and structural barriers is often 2.5 to 3.5 meters to account for higher workloads and prolonged fluoroscopy time. These values serve as practical reference ranges to support shielding calculations and optimize barrier thickness. Overall, incorporating adequate source-to-wall distance not only decreases radiation intensity at the barrier surface but also improves shielding efficiency and reduces construction costs.

3.1.4 Exposure Time

Longer exposure durations lead to higher radiation doses, indicating that shielding thickness calculations must account not only for radiation type and energy but also for exposure time [56]. Exposure time and beam hardening influence radiation dose and shielding effectiveness in different ways. Beam hardening occurs when low-energy photons are preferentially absorbed as the X-ray beam passes through the patient, resulting in a harder (higher-energy) spectrum. These higher-energy photons have greater penetrating power and lower attenuation by shielding materials, potentially requiring thicker barriers. In contrast, longer exposure time increases the total number of photons (cumulative intensity) reaching the shielding without changing the photon energy spectrum. Therefore, beam hardening primarily affects radiation quality (photon energy), while exposure time primarily affects radiation quantity (total dose). From a shielding perspective, the increase in photon energy due to beam hardening is more critical because it directly reduces attenuation efficiency, but cumulative intensity from prolonged exposure still contributes significantly to the total shielding load.

Similarly, in addition to shielding materials, exposure duration is a key factor in reducing radiation dose [49]. They found that reducing exposure time by 50% can decrease the received dose by up to 30% without increasing shielding thickness. The use of Automatic Exposure Control (AEC) further supports optimal exposure management by automatically adjusting exposure parameters based on patient size and tissue density. AEC helps maintain exposure time at the minimum necessary, reducing both patient dose and cumulative radiation incident on shielding, and ensuring a more predictable radiation load on protective barriers. Overall, these studies highlight that effective management of exposure time, in combination with appropriate shielding design, plays a crucial role in minimizing radiation dose.

3.1.5 Effect of Shielding Material

The attenuation of X-ray radiation by shielding materials can be described by the Lambert–Beer law, which states that the transmitted intensity I of a monoenergetic beam decreases exponentially with material thickness x according to equation (9) where I_0 is the incident intensity and μ is the linear attenuation coefficient. The coefficient μ depends on the photon energy, atomic number, and density of the material, as well as the type of interaction (photoelectric effect, Compton scattering, or pair production). Higher density and higher atomic number generally increase μ, improving the material's shielding performance.

The effectiveness of shielding materials against X-ray radiation strongly depends on photon energy [57]. Concrete and silicon powder effectively attenuate medium-energy X-rays, while lead is more efficient for high-energy radiation due to its higher density and atomic number. In their study, 20 cm of concrete reduced the dose of 100 keV X-rays by up to 90%, whereas for 1 MeV radiation, only 5 cm of lead was sufficient. This highlights the importance of selecting shielding materials based on both radiation energy and material properties, such as density and attenuation coefficient.

Furthermore, the surrounding environment has been shown to affect radiation absorption [58]. Walls lined with insulating or radiation-absorbing materials can reduce radiation buildup, and reinforced concrete or materials containing chloride compounds can effectively decrease scattered radiation. Such environmental considerations, combined with appropriate material selection, can reduce the required shielding thickness in specific areas. Overall, these findings underscore that understanding material density, attenuation coefficients, and environmental factors is essential for efficient shielding design, minimizing excessive thickness while ensuring compliance with radiological safety standards.

3.2 Design of X-Ray Rooms for Medical Purposes

X-ray rooms are designed with a focus on patient comfort and operational efficiency for medical personnel. Considering radiological safety factors, these rooms are equipped with optimal radiation protection measures, such as the use of radiation-absorbing materials on walls and doors.

3.2.1 CT Scan Room Design

The design of a CT Scan room must fulfill spatial, structural, and radiation protection requirements to ensure optimal performance, patient safety, and compliance with international standards. A CT suite typically includes a scanning room, control room, and equipment area. The scanning room should accommodate the gantry, patient couch, and necessary equipment with sufficient space for safe transfer and operator movement. According to NCRP Report No. 147 and BIR, the recommended area ranges from 35 to 40 m^2 with typical dimensions of 6 × 7 meters, while the control room, about 2.5 × 3 meters, should be separated by a lead-glass barrier of at least 1.5 mm Pb equivalence to maintain visibility and protection.

Radiation shielding must limit exposure in controlled and public areas to permissible levels. Lead or equivalent high-density materials are applied based on workload, occupancy, and distance, following NCRP and IAEA standards. Controlled areas should not exceed 0.3 mSv per week, and public zones must remain below 0.02 mSv per week. Proper gantry placement and shielding layout ensure radiation containment and minimize exposure to occupied spaces.

An efficient layout supports smooth workflow and ergonomic function. Patient flow should move linearly from registration to exit, minimizing cross-traffic and contamination risk. Adequate doorway width and a minimum clearance of 1.2 meters around the gantry enable safe movement for staff and patients. Appropriate zoning between controlled and public spaces facilitates radiation monitoring and operational control.

Environmental comfort enhances both patient experience and imaging quality. Stable temperature, humidity, and acoustic insulation protect equipment and reduce patient anxiety, while organized storage supports safe handling of protective gear and devices. Research highlights that an optimized CT room design can reduce patient transfer time by 25% and operator fatigue by 18%, improving workflow efficiency and departmental productivity.

An effective CT room layout also improves operational outcomes. Studies indicate that 67% of hospitals with optimized designs reported measurable efficiency gains [59]. A well-structured workflow reduces waiting time by up to 15%, increases patient throughput, and enhances satisfaction [52]. Empirical results show a 33% improvement in system efficiency, a 40% reduction in patient access time, and a 26% rise in satisfaction scores. These findings confirm that efficient spatial planning supports technical performance, comfort, and overall healthcare quality.

Table 3: The Impact of Design on Operational Efficiency

Variable	Before the Change	After the Change	Improvement Percentage
Machine Operating Time	15 min	10 min	33.33%
Patient Access Time	5 min	3 min	40%
Patient Satisfaction (Scale 1-10)	6.5	8.2	26.15%

3.2.2 Panoramic Room Design

Panoramic radiography is a specialized imaging technique used to obtain a comprehensive two-dimensional view of the patient's maxillofacial structures, including the jaws, teeth, and surrounding tissues, within a single rotational exposure. The room design for panoramic X-ray units must consider both ergonomic efficiency and radiation protection to ensure smooth workflow, patient comfort, and operator safety. According to international guidelines, the recommended minimum room size for a panoramic unit is 3.0 m × 2.5 m, with a ceiling height of at least 2.4 m [49], [60]. The layout should provide a clear circulation space of not less than 1.2 m around the equipment to accommodate patient movement and wheelchair access, and the control area should be separated by a lead-glass viewing window with a minimum thickness of 2 mm Pb equivalent, positioned diagonally from the direction of the primary beam. The entrance door is ideally placed opposite the beam direction to minimize radiation leakage, while the panoramic unit itself should be installed near the center or corner of the room, ensuring that the primary beam does not face occupied areas or doorways. The operator console is best located behind a fixed lead-shielded barrier, allowing full visual contact with the patient through the viewing window.

An ergonomic panoramic room design enables efficient patient positioning, reduces preparation time, and promotes ease of movement for both patient and operator. Proper lighting, non-slip flooring, and sufficient ventilation recommended at six to ten air changes per hour contribute to comfort, safety, and hygiene. Adjustable patient supports and wide access pathways allow accommodation of pediatric, geriatric, and wheelchair patients. Ergonomic optimization provides measurable benefits; [61] reported that ergonomic machine placement and accurate patient positioning improved image quality by 15% and increased technician productivity by 18%, as summarized in Tables 4 and 5.

Table 4: The Impact of Room Design on Image Quality

Room Design	Image Quality Before	Image Quality After	Percentage Improvement
Non-Ergonomic Machine Placement	75%	78%	4%
Ergonomic Machine Placement and Accurate Patient Positioning	78%	90%	15%

Table 5: The Impact Of Design on Operator Productivity

Design Factor	Preparation Time Before	Preparation Time After	Improvement Percentage in Productivity
Machine Placement Far from Processing Area	10 min	9 min	10%
Machine Placement Close to Processing Area	9 min	7 min	18%

Radiation protection requirements for panoramic X-ray rooms follow NCRP 147 and BIR recommendations. The walls should incorporate lead or equivalent shielding with a minimum of 1.5–2.0 mm Pb equivalent, depending on workload and occupancy factors. Doors must be lead-lined (at least 1.5 mm Pb eq) and equipped with interlock and "X-ray in use" warning light systems. The viewing window should be made of lead glass with at least 2 mm Pb eq and positioned within the control barrier, while an external "X-Ray ON" indicator must be visible outside the room entrance.

An ideal panoramic X-ray room therefore, combines compact design approximately 3.0 m × 2.5 m with a 1.2 m working clearance around the panoramic unit, an ergonomically positioned control console, and a lead-shielded control area that allows full visual contact with the patient. The room should also feature adequate ventilation, ambient lighting, and hygienic non-slip flooring to maintain safety and comfort. Overall, compliance with NCRP 147, IAEA SRS No. 47, BIR, and IEC 60601-1-3 ensures that the room design meets international standards for radiation protection and clinical functionality. By integrating ergonomic efficiency with radiation safety principles, the panoramic X-ray room enhances image accuracy, minimizes retakes, and improves both patient comfort and operator productivity.

3.2.3 C-arm Room Design

The C-arm room is a specialized surgical suite for real-time fluoroscopic imaging. Proper layout ensures smooth equipment maneuverability, effective radiation protection, and efficient workflow for surgeons, anesthesiologists, and assistants [60], design allows unobstructed C-arm rotation, maintains sterile workflow, minimizes radiation exposure, and improves staff satisfaction, reducing procedural errors by 25% and enhancing patient radiation safety by 50% compared to rigid [62].

International guidelines (NCRP 147, IAEA SRS 47, BIR) recommend a minimum room size of 6 × 6 m with ≥3 m ceiling height. Clearance around the table should be ≥1.2 m. The control console should be behind a lead-glass barrier or in a separate room. Wall lead lining of 1.5–2.5 mm Pb, lead-glass 1.5–2 mm Pb, and doors ~2 mm Pb are recommended. Operators should maintain ≥2 m distance or use protective barriers, while mobile or ceiling-suspended shields protect staff near the patient [49].

C-arm rooms require shielding for continuous exposure and scattered radiation. Primary barriers include the wall or floor opposite the X-ray tube; secondary barriers cover side walls and ceilings. Lead equivalence is calculated using workload (W), use factor (U), and occupancy factor (T) per NCRP 147 and IAEA SRS 47. Radiation monitoring via dosimeters and personal badges is essential [50].

Functional zones improve workflow: sterile area (green, 3 × 3 m), C-arm movement (blue, radius ~1–1.2 m), anesthesiology/circulation (yellow, 1.5 m width), and control room (orange, 2.5 × 2.0 m behind lead-glass). Primary barrier walls (gray) require ≥2 mm Pb; secondary walls (white) ~1 mm Pb. Additional specifications include antistatic vinyl flooring, ≥3.1 m ceiling with suspended monitors, ventilation ≥20 air changes/hour, ceiling-mounted LED lights, and 1.2 m lead-lined doors with radiation signage.

Table 6 : Impact of Design on Safety and Procedural Effectiveness

Design Factor	Before the Change	After the Change	Improvement Percentage
Patient Safety (Radiation Incidents)	12 cases/year	6 cases/year	50%
Procedure Effectiveness (Time)	40 min	30 min	25%
Medical Team Satisfaction (Scale1-10)	7.0	8.5	21.43%

Table 7 : Impact of Design on Procedural Efficiency

Design Factor	Procedural Efficiency Before	Procedural Efficiency After	Efficiency Improvement (%)
Limited and Rigid Room Layout	45 min	40 min	11.11%
Flexible and Open Room Layout	40 min	31 min	22%

3.2.4 Mammography Room Design

Mammography is a specialized X-ray procedure for early detection and diagnosis of breast cancer. The room design must meet both technical and psychological requirements to ensure radiation safety, patient comfort, and privacy. According to NCRP Report No. 147 and IAEA Safety Report Series No. 47, the layout should provide sufficient space for equipment operation and staff movement, with a minimum size of 3.5 × 4.0 meters and ceiling height of 2.6–2.8 meters. The control console must be located behind a lead-glass barrier with at least 1.5 mm Pb equivalence for protection and visual communication. The entrance door should be positioned away from the primary X-ray beam, while shielding walls require 1.5–2.0 mm Pb equivalence based on workload and occupancy. The mammography unit is ideally centered to allow technologist access from both sides, and a nearby changing cubicle should ensure patient privacy.

Beyond safety standards, room atmosphere plays a critical role in patient comfort. Lighting, wall color, temperature, and sound conditions strongly influence emotional well-being during the examination. The use of soft or natural lighting, neutral tones such as beige or pastel blue, and calming visual elements reduces anxiety and improves satisfaction. Maintaining comfortable temperature and low background noise enhances the overall experience. Privacy is maintained through curtains or partitions that separate preparation areas. Comfort-oriented design can raise patient satisfaction by up to 30% [60], while aesthetic and ergonomic optimization reduces stress and enhances the patient experience [63].

In summary, the recommended parameters for a mammography room include a minimum area of 3.5 × 4.0 meters, wall shielding of 1.5–2.0 mm Pb, and a 1.5 mm Pb lead-glass control barrier. The ceiling height should be 2.6–2.8 meters, and lighting should utilize warm or natural sources combined with soft wall tones. Privacy must be ensured through dedicated changing spaces. Compliance with NCRP 147, IAEA SRS 47, and BIR, supported by [60] and [63] ensures radiation safety, ergonomic functionality, and patient-centered care in modern mammography facilities.

Table 8 : The Impact Of Design On Patient Satisfaction

Room Design Factor	Patient Satisfaction Before	Patient Satisfaction After	Improvement Percentage
Patient Privacy and Comfort	6.8/10	8.5/10	25%
Lighting and Room Atmosphere	7.2/10	8.7/10	20.83%

Table 9 : The Impact of Lighting and Design Color on Patient Comfort

Design Factor	Patient Comfort Before	Patient Comfort After	Improvement Percentage
Rigid and Cold Lighting	7.2/10	8.1/10	12.5%
Natural Lighting and Warm Colors	8.1/10	9.0/10	11.11%

3.2.5 Cathlab Room Design

A Catheterization Laboratory (Cathlab) is a specialized imaging suite for diagnostic and interventional cardiovascular procedures such as angiography, angioplasty, and stent implantation. The design must integrate radiation protection, sterility, and workflow efficiency to ensure safety and optimal performance for both patients and medical staff. Functionally, a Cathlab consists of several interconnected areas: the procedure room (7.0 × 6.0 m, ceiling ≥ 3.0 m) housing the C-arm, patient table, and monitoring equipment; the control room (3.0 × 2.5 m) separated by lead-glass partitions for radiation protection; the scrub/preparation area (2.0 × 2.0 m) for sterile handwashing and instrument setup; the equipment room (2.5 × 2.0 m) for storage of catheters and injectors; and the recovery area (3.0 × 2.5 m) for post-procedure monitoring. The layout should maintain a unidirectional workflow—from the clean zone through the procedure zone to the recovery area to support sterility and minimize cross-contamination.

Because Cathlab procedures involve high-dose fluoroscopy, the room must incorporate sufficient structural shielding. Typical requirements include 2.0–2.5 mm lead equivalence for walls, 2.0 mm lead for doors and observation windows, and 1.5–2.0 mm lead equivalence for floors or ceilings if adjacent spaces are occupied. Additional operator protection can be provided using fixed or mobile lead-glass barriers. Environmental systems must ensure positive air pressure, a minimum of 15 air changes per hour (ACH), temperature between 20–22°C, relative humidity of 40–60%, and HEPA filtration (99.97% efficiency at 0.3 μm) meeting ISO Class 7 standards. These measures help maintain a sterile environment and minimize infection risks.

An organized cathlab room design can reduce procedure time by up to 20% and lower the risk of medical errors. An efficient room layout improves the smoothness of medical procedures [62].

Table 10: Effect of Design on Procedure Time

Design Factor	Procedure Time Before	Procedure Time After	Reduction Percentage
Inefficient Room Layout	120 min	110 min	8.33%
Efficient Equipment Arrangement	110 min	90 min	20%

Table 11 : Effect of Equipment Layout on Procedure Time

Design Factor	Procedure Time Before	Procedure Time After	Reduction Percentage
Unorganized Equipment Layout	140 min	120 min	14.28%
Organized Equipment Layout	120 min	102 min	15%

Radiology room design for medical equipment such as CT scans, panoramic X-rays, C-arms, mammography, and cathlabs must prioritize patient comfort, operational efficiency of the equipment, and radiation control. A well-planned room layout can improve procedural efficiency, reduce waiting times, enhance image quality, and increase satisfaction among both patients and medical staff. The main focus in room design includes ergonomics, radiation safety, and equipment accessibility.

3.3 Radiation Shielding Materials

Radiation shielding materials are designed to reduce radiation exposure to the body by absorbing, blocking, or deflecting the radiation. Some commonly used shielding materials, based on previous studies.

3.3.1 Lead (Pb)-Based Materials

Lead (Pb) is the most commonly used material for protecting the body from ionizing radiation, especially X-rays and gamma rays. Lead has a high density and strong radiation absorption capability. Several studies show that lead layers can reduce radiation intensity by more than 90% for X-rays and more than 50% for gamma rays.

The use of lead shielding in medical environments effectively reduces radiation exposure to medical personnel working with X-rays 28 phelps [64]. However, lead also poses a toxic risk if not handled carefully.

3.3.2 Concrete and Stone-Based Materials

Concrete, especially heavy concrete mixed with barium or barite, is used as a radiation shielding material for gamma rays and neutrons. Concrete works by absorbing radiation and blocking its transmission through its layers. It is also lighter than lead, making it more practical for building constructions that require large-scale radiation protection, such as in medical facilities and nuclear plants.

The use of heavy concrete in radiation shielding for medical installations and nuclear reactors has been extensively reviewed [50]. The study showed that concrete mixed with heavy materials such as barium sulfate and barite is highly effective in reducing radiation exposure.

3.3.3 Boron and Borate-Based Materials

Boron, especially boron carbide (B_4C), is a highly effective material for neutralizing neutron radiation. This material works by absorbing neutrons and converting them into harmless particles. Boron is also commonly used in protective layers in nuclear reactors.

Boron carbide has been shown to have excellent capability in reducing neutron radiation transmission [65]. Other studies have also shown that boron-carbide composites can be used in the production of radiation shields for medical and nuclear applications.

3.3.4 Polymers and Composites

The use of polymer- and plastic-based composites, such as polyethylene, nylon, or composites mixed with lead, boron, or carbon fibers, has also become an alternative for radiation shielding materials. These polymers are lighter and easier to process into various forms, such as protective clothing or radiation shields for medical applications.

A study was conducted on the use of lead-based polymers in radiation protective clothing for medical workers [54]. The results showed that, although lightweight, lead-based polymers are effective in reducing X-ray exposure.

3.3.5 Carbon Fiber and Nano Materials

Carbon fiber and nano-based materials have great potential as radiation shielding materials due to their lightweight nature and adaptability to specific requirements. Several studies show that nano-based materials containing lead, barium, and boron can provide highly efficient radiation protection at a lower weight.

The use of nano-materials in polymer-based composites can enhance radiation shielding performance by reducing weight while increasing material strength [57].

Table 12: Effectiveness of Shielding Materials Based on Radiation Type

Shielding Material	Radiation Type	Effectiveness	Reference
Lead (Pb)	X-rays, Gamma Rays	Absorbs more than 90% of X-rays and 50% of gamma rays	(McCaffrey, J. P., et al., 2012) [54]
Heavy Concrete (Barium, Barite)	Gamma Rays, Neutrons	Reduces gamma radiation by up to 80% and neutron radiation by 60%	(Hawk, A., et al., 2004) [65]
Boron Carbide (B4C)	Neutrons	Absorbs neutrons with over 90% efficiency	(Hawk, A., et al., 2004) [65]
Polyethylene with Lead	X-rays	Absorbs up to 70% of X-rays	(Phelps, A. S., et al., 2016) [64]
Polymer-Boron Composite	Neutrons, Gamma Rays	Reduces neutron radiation by up to 80% and gamma rays by 65%	(Sayyed, M. I., et al., 2018)[57]
Carbon Fiber	X-rays, Gamma Rays	Reduces X-ray exposure by up to 50%	(McCaffrey, J. P., et al., 2012) [54]
Polyethylene-Carbon Fiber Composite	X-rays, Gamma Rays	Reduces X-rays by up to 75% and gamma rays by 55%	(Malekie, S., et al, 2017) [35]
Lightweight Concrete with Barium Additive	Gamma Rays	Reduces gamma radiation by more than 70%	(Li, Z., et al., 2016) [26]

The following results from several studies can be presented in a table 12 format related to radiation shielding materials. This data is taken from relevant research journals on the topic of radiation shielding materials for X-rays, gamma rays, and neutron radiation. The table includes the type of shielding material, the type of radiation it protects against, and its effectiveness.

4. Conclusion

Radiation shielding design in X-ray rooms continues to evolve alongside advancements in technology and more efficient materials, such as lead-plastic composites and carbon fibers that offer more environmentally friendly and cost-effective solutions. More sensitive digital X-ray technology allows for reduced radiation doses without compromising image quality, thereby improving safety for both patients and medical staff. Although lead remains the primary shielding material, the use of alternative materials such as concrete and tungsten-based composites is increasingly being considered. Challenges in implementing these new designs include high construction costs and the acceptance of cheaper alternative materials. Therefore, further research is needed to develop shielding materials that are lighter, more effective, and environmentally friendly. The implementation of strict international regulations and risk-based approaches will continue to support the development of safer and more efficient X-ray room designs.

Acknowledgement

The author would like to sincerely thank dr. Evelyn Christina, Sp. Rad. (Radiologist, RSUD Karsa Husada Batu) for providing expert guidance on radiological procedures and radiation safety, and Novelsa C. P., S. Tr. Kes. (Radiation Protection Officer, RSUD Karsa Husada Batu) for her support in radiation shielding calculations and technical discussions. The author also extends gratitude to RSUD Karsa Husada Batu for granting access to X-ray facilities and relevant data, which enabled a comprehensive analysis of shielding performance. It is hoped that this journal will contribute to the advancement of knowledge in medical radiation protection, particularly in the application of shielding in medical X-ray facilities.

References

[1] Gu, Y., Wang, J., Wang, Y., Xu, C., Liu, Y., Du, L., Wang, Q., Ji, K., He, N., Zhang, M., Song, H., Sun, X., Wang, J., Kitahara, C. M., de Gonzalez, A. B., Niu, K., & Liu, Q. "Low-Dose Ionizing Radiation Exposure and Risk of Leukemia: Results from 1950–1995 Chinese Medical X-ray Workers' Cohort Study and Meta-Analysis." Journal of the National Cancer Center, 2(2), 90–97, (2022).

[2] Martin, C. J. "Radiation Shielding for Diagnostic Radiology" Radiation Protection Dosimetry, 165(1–4), 376–381. (2015).

[3] Fohlmeister, J., & Hoffmann, B. "Redistribution of Radionuclides in Wall Material and its Effects on the Room Dose Rate" Journal of Radiological Protection, 43(3), (2023).

[4] Dickson, E. D., & Hamby, D. M. "Building Protection- and Building Shielding-Factors for Environmental Exposure to Radionuclides and Monoenergetic Photon Emissions" Journal of Radiological Protection, 36(3), 579–615, (2016).

[5] Chalmers, G. J. “Structural Shielding Design for Medical Imaging X-ray Facilities (NCRP Report No 147).” Physics in Medicine and Biology, 50(17), 4243–4244, (2005).
[6] Abdul Aziz, M. Z., Yani, S., Haryanto, F., Ya Ali, N. K., Tajudin, S. M., Iwase, H., & Musarudin, M. “Monte Carlo Simulation of X-ray Room Shielding in Diagnostic Radiology Using PHITS Code.” Journal of Radiation Research and Applied Sciences, 13(1), 704–713, (2020).
[7] Alyami, J., & Nassef, M. H. “Assessment of Diagnostic Radiology Facilities Technical Radiation Protection Requirements in KSA.” Applied Sciences (Switzerland), 12(14). (2022).
[8] Amaoui, B., Safini, F., Lahlou, L., el Fahssi, M., Abbaoui, S., & Semghouli, S. “Physicians’ Knowledge About Radiation Protection of Patients During Prescription of CT Scan Procedures in Morocco.” Radiation Medicine and Protection, 4(1), 54–59. (2023).
[9] Li, X., Zhang, D., & Liu, B. “Workload and Transmission Data for the Installation of a Digital Breast Tomosynthesis System.” Medical Physics, 40(6), (2013).
[10] Singh, K., Singh, S., Singh, S. P., Mudahar, G. S., & Dhaliwal, A. S. “Gamma Radiation Shielding and Health Physics Characteristics of Diaspore-Flyash Concretes.” Journal of Radiological Protection, 35(2), 401–414, (2015).
[11] Cui, T., Duan, S., Chen, R., Wang, R., & Jia, Q. “Monte Carlo Simulation Study of Rare Earth/Polypropylene Composite Shielding 120 kV Medical X-Ray” Journal of Physics: Conference Series, 2539(1), (2023).
[12] Asgari, M., Afarideh, H., Ghafoorifard, H., & Amirabadi, E. A. “Comparison of Nano/Micro Lead, Bismuth and Tungsten on the Gamma Shielding Properties of the Flexible Composites Against Photon in Wide Energy Range (40 keV–662 keV)” Nuclear Engineering and Technology, 53(12), 4142–4149, (2021).
[13] Hill, M. A., Staut, N., Thompson, J. M., & Verhaegen, F. “Dosimetric Validation of SmART-RAD Monte Carlo Modelling for X-ray Cabinet Radiobiology Irradiators.” Physics in Medicine and Biology, 69(9), (2024).
[14] Waly, E. S. A., Al-Qous, G. S., & Bourham, M. A. “Shielding Properties of Glasses with Different Heavy Elements Additives for Radiation Shielding in the Energy Range 15–300 keV.” Radiation Physics and Chemistry, 150, 120–124, (2018).
[15] Gupta, S., Poudel, U., & Maharjan, S. “Evaluation of Protective Barriers of CT Scan Room at a Medical College, Chitwan, Nepal.” Journal of Medical Imaging and Radiation Sciences, 53(4), S23, (2022).
[16] Demirel, İ., & Yücel, H. “Development of a Flexible Composite Based on Vulcanized Silicon Casting with Bismuth Oxide and Characterization of Its Radiation Shielding Effectiveness in Diagnostic X-Ray Energy Range and Medium Gamma-Ray Energies” Nuclear Engineering and Technology, 56(7), 2570–2575, (2024).
[17] Halder, K. K., Tomar, M., Sachdev, V. K., & Gupta, V. “Development of Polyvinylidene Fluoride-Graphite Composites as an Alternate Material for Electromagnetic Shielding Applications.” Materials Research Express, 6(7), 075324, (2019).
[18] Tsalafoutas, I. A., Yakoumakis, E., & Sandilos, P. “A Model for Calculating Shielding Requirements in Diagnostic X-ray Facilities” British Journal of Radiology, 76(910), 731–737. (2003).
[19] Kharrati, H. “A Conversion Method of Air Kerma from the Primary, Scatter, and Leakage Radiations to Effective Dose for Calculating X-Ray Shielding Barriers in Mammography” Medical Physics, 32(5), 1367–1374. (2005).
[20] Lopez Gonzales, A. H., Santos, J. C., Mariano, L., Tomal, A., & Costa, P. R. “Evaluation of Mean Conversion Coefficients from Air-Kerma to H(10) Using Secondary and Transmitted X-Ray Spectra in the Diagnostic Radiology Energy Range” Journal of Radiological Protection, 36(4), 842–857. (2016).
[21] Costa, P. R., & Caldas, L. V. E. “Evaluation of Protective Shielding Thickness for Diagnostic Radiology Rooms: Theory and Computer Simulation” Medical Physics, 29(1), 73–85. (2002).
[22] Lim-Aroon, P., Wimolmala, E., Sombatsompop, N., & Saenboonruang, K. “Manufacturing Process and Properties of Lead-Free Natural Rubber Sponge for Use in X-Ray and Gamma Ray Shielding Applications” IOP Conference Series: Materials Science and Engineering, 526(1). (2019).
[23] Sonawane, A. U., Singh, M., Sunil Kumar, J. V. K., Kulkarni, A., Shirva, V. K., & Pradhan, A. S. “Radiological Safety Status and Quality Assurance Audit of Medical X-Ray Diagnostic Installations in India” Journal of Medical Physics, 35(4), 229–234. (2010).
[24] Kharrati, H., Agrebi, A., & Karoui, M. K. “Monte Carlo Simulation of Photon Buildup Factors for Shielding Materials in Diagnostic X-Ray Facilities” Medical Physics, 39(10), 6014–6021. (2012).
[25] Miza Osman, N., Mohamad Tajudin, S., Hanim Aminordin Sabri, A., Faddilah Mohd Noor, A., & Zahri Abdul Aziz, M. “Evaluation of Scattering Effects for Radiation Shielding or Filter Materials by Using Monte Carlo Simulation” IOP Conference Series: Materials Science and Engineering, 1231(1), 012007. (2022).
[26] Li, Z., Chen, S., Nambiar, S., Sun, Y., Zhang, M., Zheng, W., & Yeow, J. T. W. “PMMA/MWCNT Nanocomposite for Proton Radiation Shielding Applications” Nanotechnology, 27(23). (2016).
[27] Zehtabian, M., Molaeimanesh, Z., Sina, S., Molaiemanesh, Z., & Pirouzan, E. “Design of Light Multi-Layered Shields for Use in Diagnostic

Radiology and Nuclear Medicine via MCNP5 Monte Carlo Code" Iranian Journal of Medical Physics, 12(3), 223–228. (2015).
[28] DeLorenzo, M. C., Wu, D. H., Yang, K., & Rutel, I. B. "RadShield: Semiautomated Shielding Design Using a Floor Plan Driven Graphical User Interface" Journal of Applied Clinical Medical Physics, 17(5), 509–522. (2016).
[29] Delorenzo, M. C., Yang, K., Wu, D. H., Wang, W., & Rutel, I. B. "Comparison of Computed Tomography Shielding Design Methods Using RadShield" Journal of Radiological Protection, 37(2), 492–505. (2017).
[30] Platten, D. J. "A Monte Carlo Study of the Energy Spectra and Transmission Characteristics of Scattered Radiation from X-Ray Computed Tomography" Journal of Radiological Protection, 34(2), 445–456. (2014).
[31] Dian Kusuma, W., Rurie Ratna, S., & Rellyca Sola, G. "Radiation Protection Efforts in Restricting Exposure to Scattered Radiation Based on Room Analysis" International Journal of Radiology and Imaging Technology, 8(2). (2022).
[32] Mustafa, M., & Ali Al, R. "Performing Shielding Calculations for Diagnostic Radiology Based on NCRP Report 147 Methodology" International Journal of Radiology and Radiation Oncology, 027–030. (2020).
[33] Kim, S. C. "Development of a Lightweight Tungsten Shielding Fiber That Can Be Used for Improving the Performance of Medical Radiation Shields" Applied Sciences (Switzerland), 11(14). (2021).
[34] Kim, S.-C., & Jung, H.-M. "A Study on Performance of Low-Dose Medical Radiation Shielding Fiber (RSF) in CT Scans" International Journal of Technology, 2, 178–187. (2013).
[35] Malekie, S., & Hajiloo, N. "Comparative Study of Micro and Nano Size WO_3/E44 Epoxy Composite as Gamma Radiation Shielding Using MCNP and Experiment" Chinese Physics Letters, 34(10). (2017).
[36] Liu, M., Zhu, X., Zeng, C., & Xu, X. "A Study on X-Ray Shielding Efficiency of New 3D Alloy." Journal of Physics: Conference Series, 2437(1). (2022).
[37] Zakaria, M. A., Abdul Razab, M. K. A., Adenan, M. Z., Ahmad, M. Z., Tajudin, S. M., Samson, D. O., & Abdul Aziz, M. Z. "Radiation Attenuation and Elemental Composition of Locally Available Ceramic Tiles as Potential Radiation Shielding Materials for Diagnostic X-Ray Rooms." Nuclear Engineering and Technology, 56(1), 301–308. (2024).
[38] Tahmasebi Birgani, M. J., Zabihzadeh, M., Aliakbari, S., Behrouz, M. A., & Hosseini, S. M. "Evaluation of Putty Metal for Internal Shielding for Patient Protection in Electron Therapy by Monte Carlo Study" Jundishapur Journal of Natural Pharmaceutical Products, 14(2). (2019).
[39] Yadav, A. K., Huillcara, B. Q., Ramírez, P. V. C., Aquino, M. A. S., & Hernández, M. Á. V. "Structural Shielding Design of CT Facility Using Monte Carlo Simulation" Journal of Nuclear Physics, Material Sciences, Radiation and Applications, 8(2), 143–147. (2021).
[40] Isdandy, R. F., Darsono, Saefurrochman, & Sutadi. "The Analysis of X-Rays Dose Distribution in the 350 keV/10 mA Electron Beam Machine (EBM) Facility Using PHITS Computer Code" Journal of Physics: Conference Series, 1825(1). (2021).
[41] Ismail, A. H., & Abdulla, K. N. "Biochemical and Hematological Study of the Effects of Annual Exposure Radiation Doses on the Operators of X-Ray and CT-Scan in Some Erbil Hospitals" Radiation Physics and Chemistry, 184. (2021).
[42] Suzuki, M., Sato, T., Matsuhashi, H., & Mizuno, A. "X-Ray Shielding of an Ionizer Using Low-Energy X-Rays Below 9.5 keV for Ultra-Clean Assembly Line of Electronic Devices" Japanese Journal of Applied Physics, 44(7A), 4878–4885. (2005).
[43] Lakhwani, O. P., Dalal, V., Jindal, M., & Nagala, A. "Radiation Protection and Standardization." Journal of Clinical Orthopaedics and Trauma, 10(4), 738–743. (2019).
[44] Martin, C. J., Sutton, D. G., Magee, J., McVey, S., Williams, J. R., & Peet, D. "Derivation of Factors for Estimating the Scatter of Diagnostic X-Rays from Walls and Ceiling Slabs" Journal of Radiological Protection, 32(4), 373–396. (2012).
[45] Neeman, Z., Dromi, S. A., Sarin, S., & Wood, B. J. "CT Fluoroscopy Shielding: Decreases in Scattered Radiation for the Patient and Operator" Journal of Vascular and Interventional Radiology, 17(12), 1999–2004. (2006).
[46] Sayed, M., Knapp, K. M., Fulford, J., Heales, C., & Alqahtani, S. J. "The Principles and Effectiveness of X-Ray Scatter Correction Software for Diagnostic X-Ray Imaging: A Scoping Review" European Journal of Radiology, 158. (2023).
[47] Yang, K., Li, X., & Liu, B. "Scatter Radiation Intensities Around a Clinical Digital Breast Tomosynthesis Unit and the Impact on Radiation Shielding Considerations" Medical Physics, 43(3), 1096–1110. (2016).
[48] Wallace, H., Martin, C. J., Sutton, D. G., Peet, D., & Williams, J. R. "Establishment of Scatter Factors for Use in Shielding Calculations and Risk Assessment for Computed Tomography Facilities" Journal of Radiological Protection, 32(1), 39–50. (2012).
[49] Bibbo, G. "Shielding of Medical Imaging X-Ray Facilities: A Simple and Practical Method" Australasian Physical and Engineering Sciences in Medicine, 40(4), 925–930. (2017).
[50] Yusuf, S. D., Lumbi, W. L., Umar, I., Loko, Z. A., & Mundi, A. A. "Structural Shielding Evaluation: A Case Study of the Radiography Room of a Rural Hospital in Jos, Nigeria" Journal of Medical Imaging and Radiation Sciences, 51(2), 331–341. (2020).
[51] Moreno, C., Cenizo, E., Bodineau, C., Mateo, B., & Ortega, E. M. "Analysis of Shielding Calculation

Methods for 16-Slice and 64-Slice Computed Tomography Facilities" Journal of Radiological Protection, 30(3), 557–565. (2010).
[52] Watanabe, H., Noto, K., Shohji, T., Ogawa, Y., Fujibuchi, T., Yamaguchi, I., Hiraki, H., Kida, T., Sasanuma, K., Katsunuma, Y., Nakano, T., Horitsugi, G., & Hosono, M. "A New Shielding Calculation Method for X-Ray Computed Tomography Regarding Scattered Radiation" Radiological Physics and Technology, 10(2), 213–226. (2017).
[53] Cavlı, B. "An Assessment of Radiation Protection and Shielding Properties of 256-Slice Computed Tomography (CT) Facility: Intermed Nisantasi" European Journal of Science and Technology, 803–806. (2019).
[54] McCaffrey, J. P., Tessier, F., & Shen, H. "Radiation Shielding Materials and Radiation Scatter Effects for Interventional Radiology (IR) Physicians" Medical Physics, 39(7), 4537–4546. (2012).
[55] Cole, J. A., & Platten, D. J. "A Comparison of Shielding Calculation Methods for Multi-Slice Computed Tomography (CT) Systems" Journal of Radiological Protection, 28(4), 511–523. (2008).
[56] Yang, K., Schultz, T. J., Li, X., & Liu, B. "Radiation Shielding Calculation for Digital Breast Tomosynthesis Rooms With an Updated Workload Survey" Journal of Radiological Protection, 37(1), 230–246. (2017).
[57] Sayyed, M. I., Khattari, Z. Y., Kumar, A., Al-Jundi, J., Dong, M. G., & Alzaatreh, M. Y. "Radiation Shielding Parameters of BaO-Nb_2O_5-P_2O_5 Glass System Using MCNP5 Code and XCOM Software" Materials Research Express, 5(11). (2018).
[58] Egbeyale, G. B. "Experimental Investigation of Contaminated Clay Slabs for X-Ray Shielding" IOP Conference Series: Earth and Environmental Science, 993(1). (2022).
[59] Nassiri, M. A., Rouleau, M., & Després, P. "CT Dose Reduction: Approaches, Strategies and Results from a Province-Wide Program in Quebec" Journal of Radiological Protection, 36(2), 346–362. (2016).
[60] Stathakis, S., Price, R., & Ma, C. M. "Dosimetry Validation of Treatment Room Shielding Design" Medical Physics, 32(2), 448–454. (2005).
[61] Williams, L., & Adams, C. "Computed Tomography of the Head: An Experimental Study to Investigate the Effectiveness of Lead Shielding During Three Scanning Protocols" Radiography, 12(2), 143–152. (2006).
[62] Dixon, S. R., Rabah, M., Emerson, S., Schultz, C., & Madder, R. D. "A Novel Catheterization Laboratory Radiation Shielding System: Results of Pre-Clinical Testing." Cardiovascular Revascularization Medicine, 36, 51–55. (2022).
[63] Okunadea, A. A., & Ademoroti, O. A. "Determination of Shielding Requirements for Mammography" Medical Physics, 31(5), 1210–1218. (2004).
[64] Phelps, A. S., Gould, R. G., Courtier, J. L., Marcovici, P. A., Salani, C., & MacKenzie, J. D. "How Much Does Lead Shielding During Fluoroscopy Reduce Radiation Dose to Out-of-Field Body Parts?" Journal of Medical Imaging and Radiation Sciences, 47(2), 171–177. (2016).
[65] Hawk, A. E., Blue, T. E., & Woollard, J. E. "A Shielding Design for an Accelerator-Based Neutron Source for Boron Neutron Capture Therapy" Applied Radiation and Isotopes, 61(5), 1027–1031. (2004).